

A Search for Nonresonant $B^+ \rightarrow h^+ h^- h^+$ Decays

T. Bergfeld,¹ B. I. Eisenstein,¹ J. Ernst,¹ G. E. Gladding,¹ G. D. Gollin,¹ E. Johnson,¹ I. Karliner,¹ M. Palmer,¹ M. Selen,¹ J. J. Thaler,¹ K. W. Edwards,² A. Bellerive,³ D. I. Britton,³ R. Janicek,³ D. B. MacFarlane,³ K. W. McLean,³ P. M. Patel,³ A. J. Sadoff,⁴ R. Ammar,⁵ P. Baringer,⁵ A. Bean,⁵ D. Besson,⁵ D. Coppage,⁵ C. Darling,⁵ R. Davis,⁵ N. Hancock,⁵ S. Kotov,⁵ I. Kravchenko,⁵ N. Kwak,⁵ S. Anderson,⁶ Y. Kubota,⁶ M. Lattery,⁶ J. J. O'Neill,⁶ S. Patton,⁶ R. Poling,⁶ T. Riehle,⁶ A. Smith,⁶ V. Savinov,⁶ M. S. Alam,⁷ S. B. Athar,⁷ Z. Ling,⁷ A. H. Mahmood,⁷ H. Severini,⁷ S. Timm,⁷ F. Wappler,⁷ A. Anastassov,⁸ S. Blinov,^{8,*} J. E. Duboscq,⁸ R. Fulton,⁸ D. Fujino,⁸ K. K. Gan,⁸ T. Hart,⁸ K. Honscheid,⁸ H. Kagan,⁸ R. Kass,⁸ J. Lee,⁸ M. Sung,⁸ A. Undrus,^{8,*} R. Wanke,⁸ A. Wolf,⁸ M. M. Zoeller,⁸ B. Nemati,⁹ S. J. Richichi,⁹ W. R. Ross,⁹ P. Skubic,⁹ M. Wood,⁹ M. Bishai,¹⁰ J. Fast,¹⁰ E. Gerndt,¹⁰ J. W. Hinson,¹⁰ D. H. Miller,¹⁰ E. I. Shibata,¹⁰ I. P. J. Shipsey,¹⁰ M. Yurko,¹⁰ L. Gibbons,¹¹ S. D. Johnson,¹¹ Y. Kwon,¹¹ S. Roberts,¹¹ E. H. Thorndike,¹¹ C. P. Jessop,¹² K. Lingel,¹² H. Marsiske,¹² M. L. Perl,¹² S. F. Schaffner,¹² D. Ugolini,¹² R. Wang,¹² X. Zhou,¹² T. E. Coan,¹³ V. Fadeyev,¹³ I. Korolkov,¹³ Y. Maravin,¹³ I. Narsky,¹³ V. Shelkov,¹³ R. Stroynowski,¹³ J. Staeck,¹³ I. Volobouev,¹³ J. Ye,¹³ M. Artuso,¹⁴ A. Efimov,¹⁴ M. Gao,¹⁴ M. Goldberg,¹⁴ R. Greene,¹⁴ F. Frasconi,¹⁴ D. He,¹⁴ S. Kopp,¹⁴ G. C. Moneti,¹⁴ R. Mountain,¹⁴ Y. Mukhin,¹⁴ S. Schuh,¹⁴ T. Skwarnicki,¹⁴ S. Stone,¹⁴ X. Xing,¹⁴ J. Bartelt,¹⁵ S. E. Csorna,¹⁵ V. Jain,¹⁵ S. Marka,¹⁵ A. Freyberger,¹⁶ R. Godang,¹⁶ D. Gibaut,¹⁶ K. Kinoshita,¹⁶ I. C. Lai,¹⁶ P. Pomianowski,¹⁶ S. Schrenk,¹⁶ G. Bonvicini,¹⁷ D. Cinabro,¹⁷ L. Perera,¹⁷ B. Barish,¹⁸ M. Chadha,¹⁸ S. Chan,¹⁸ G. Eigen,¹⁸ J. S. Miller,¹⁸ C. O'Grady,¹⁸ M. Schmittler,¹⁸ J. Urheim,¹⁸ A. J. Weinstein,¹⁸ F. Würthwein,¹⁸ D. M. Asner,¹⁹ D. W. Bliss,¹⁹ W. S. Brower,¹⁹ G. Masek,¹⁹ H. P. Paar,¹⁹ J. Gronberg,²⁰ C. M. Korte,²⁰ D. J. Lange,²⁰ R. Kutschke,²⁰ S. Menary,²⁰ R. J. Morrison,²⁰ S. Nakanishi,²⁰ H. N. Nelson,²⁰ T. K. Nelson,²⁰ C. Qiao,²⁰ J. D. Richman,²⁰ D. Roberts,²⁰ A. Ryd,²⁰ H. Tajima,²⁰ M. S. Witherell,²⁰ R. Balest,²¹ B. H. Behrens,²¹ K. Cho,²¹ W. T. Ford,²¹ H. Park,²¹ P. Rankin,²¹ J. Roy,²¹ J. G. Smith,²¹ J. P. Alexander,²² C. Bebek,²² B. E. Berger,²² K. Berkelman,²² K. Bloom,²² D. G. Cassel,²² H. A. Cho,²² D. M. Coffman,²² D. S. Crowcroft,²² M. Dickson,²² P. S. Drell,²² R. Ehrlich,²² R. Elia,²² A. D. Foland,²² P. Gaidarev,²² B. Gittelman,²² S. W. Gray,²² D. L. Hartill,²² B. K. Heltsley,²² P. I. Hopman,²² S. L. Jones,²² J. Kandaswamy,²² N. Katayama,²² P. C. Kim,²² D. L. Kreinick,²² T. Lee,²² Y. Liu,²² G. S. Ludwig,²² J. Masui,²² J. Mevissen,²² N. B. Mistry,²² C. R. Ng,²² E. Nordberg,²² M. Ogg,^{22,†} J. R. Patterson,²² D. Peterson,²² D. Riley,²² A. Soffer,²² C. Ward,²² P. Avery,²³ M. Athanas,²³ C. D. Jones,²³ M. Lohner,²³ C. Prescott,²³ S. Yang,²³ J. Yelton,²³ J. Zheng,²³ G. Brandenburg,²⁴ R. A. Briere,²⁴ D. Y.-J. Kim,²⁴ T. Liu,²⁴ M. Saulnier,²⁴ R. Wilson,²⁴ H. Yamamoto,²⁴ T. E. Browder,²⁵ F. Li,²⁵ Y. Li,²⁵ and J. L. Rodriguez²⁵

(CLEO Collaboration)

¹University of Illinois, Champaign-Urbana, Illinois 61801

²Carleton University, Ottawa, Ontario, Canada K1S 5B6
and the Institute of Particle Physics, Canada

³McGill University, Montréal, Québec, Canada H3A 2T8
and the Institute of Particle Physics, Canada

⁴Ithaca College, Ithaca, New York 14850

⁵University of Kansas, Lawrence, Kansas 66045

⁶University of Minnesota, Minneapolis, Minnesota 55455

⁷State University of New York at Albany, Albany, New York 12222

⁸Ohio State University, Columbus, Ohio 43210

⁹University of Oklahoma, Norman, Oklahoma 73019

¹⁰Purdue University, West Lafayette, Indiana 47907

¹¹University of Rochester, Rochester, New York 14627

¹²Stanford Linear Accelerator Center, Stanford University, Stanford, California 94309

¹³Southern Methodist University, Dallas, Texas 75275

¹⁴Syracuse University, Syracuse, New York 13244

¹⁵Vanderbilt University, Nashville, Tennessee 37235

¹⁶Virginia Polytechnic Institute and State University, Blacksburg, Virginia 24061

¹⁷Wayne State University, Detroit, Michigan 48202

¹⁸California Institute of Technology, Pasadena, California 91125

¹⁹University of California, San Diego, La Jolla, California 92093

²⁰University of California, Santa Barbara, California 93106

²¹University of Colorado, Boulder, Colorado 80309-0390

²²Cornell University, Ithaca, New York 14853

²³University of Florida, Gainesville, Florida 32611

²⁴Harvard University, Cambridge, Massachusetts 02138

²⁵University of Hawaii at Manoa, Honolulu, Hawaii 96822

(Received 23 August 1996)

We use data collected by the CLEO II detector at the Cornell Electron Storage Ring (CESR) to search for $B^+ \rightarrow h^+ h^- h^+$ (nonresonant) decays, where h^\pm can be either π^\pm , K^\pm , or $p(\bar{p})$. We see no evidence for signals and set upper limits on the branching fractions in the range $(2.8\text{--}8.9) \times 10^{-5}$. If observed, these decays may display CP violating asymmetries. [S0031-9007(96)01781-4]

PACS numbers: 13.25.Hw, 14.40.Nd

The mode $B^+ \rightarrow (h^+ h^-) h^+$, where h^\pm can be either π^\pm , K^\pm , or $p(\bar{p})$, may display CP violating asymmetries when $(h^+ h^-)$ pairs have masses near the η_c or χ_{c0} resonances [1]. This is because the large decay widths of the η_c and χ_{c0} resonances (10–15 MeV) provide a large strong phase difference (expected to be $\pi/2$) between the two contributions to the decay amplitude; one due to the decay proceeding via the $\bar{b} \rightarrow \bar{c} c \bar{d}$ transition producing $\eta_c(\chi_{c0})\pi^\pm$ and the other due to the $\bar{b} \rightarrow \bar{u} u \bar{d}$ transition producing nonresonant states like $\pi^+ \pi^- \pi^\pm$ or $K^+ K^- \pi^\pm$. These two contributions also have different weak phases, thus leading to a CP asymmetry. Asymmetries of the order of 10% are expected in some of these modes.

The branching ratio for $B^+ \rightarrow \pi^+ \pi^+ \pi^-$ (nonresonant) is predicted to be in the range $(1.5\text{--}8.4) \times 10^{-5}$ [2]. The authors of Ref. [2] point out that the interference between the nonresonant amplitude [with $m(\pi^+ \pi^-) \approx 3.4$ GeV] and $B^+ \rightarrow \chi_{c0} \pi^+$ followed by $\chi_{c0} \rightarrow \pi^+ \pi^-$ could lead to a measurable CP asymmetry of about $(0.40\text{--}0.48) \sin \gamma$, where $\gamma = \arg(V_{ub}^*)$ [3]. This is an example of a process in which one may be able to cleanly measure γ at an $e^+ e^-$ facility operating at the $Y(4S)$.

This paper describes a search for $B^+ \rightarrow \pi^+ \pi^+ \pi^-$ (nonresonant), as well as the other nonresonant states $B^+ \rightarrow \pi^+ \pi^- K^+$, $\pi^+ \pi^+ K^-$, $\pi^+ K^- K^+$, $K^+ K^+ K^-$, $p \bar{p} \pi^+$, and $p \bar{p} K^+$, and their charge conjugates.

The data used in this analysis were recorded by the CLEO II detector operating at the Cornell Electron Storage Ring (CESR). The dataset consists of approximately 3.17 fb^{-1} of $e^+ e^-$ collisions on the $Y(4S)$ and 1.14 fb^{-1} in the continuum [60 MeV below the $Y(4S)$]. The CLEO II detector is described elsewhere [4].

Pions, kaons, and protons are identified using specific ionization information collected by the central tracking chambers. For pions and kaons, we require that dE/dx measurements be within 2.5σ of the expected hypothesis. For tracks above 1 GeV/c, approximately 98% of true pions and kaons pass this cut. For the same momentum range, the probability for a kaon to fake a pion (and vice versa) is about 87%, and the probability for a proton to fake a pion or a kaon is about 75%. For protons, we calculate the ratio of the probability of the track to be a proton and the sum of the probabilities of the track to be a π , K or a proton, and require this ratio to be greater than 0.25. For tracks with momentum above 1 GeV/c, approximately

87% of true protons pass this requirement, whereas about (30–70)% of π 's and K 's pass this cut (depending upon the π/K momenta). These results indicate that dE/dx measurements provide some discrimination between pions, kaons, and protons. Additional separation is provided by energy constraints (discussed below).

The main background in this analysis is due to the continuum under the $Y(4S)$. Such backgrounds are suppressed using event shape cuts. We require that events have $R_2 = H_2/H_0 < 0.3$, where H_2 and H_0 are the Fox-Wolfram moments [5]. The R_2 distribution for $B\bar{B}$ events produced at the $Y(4S)$ peaks toward zero, while for jetlike continuum events it peaks toward one. In addition, we require $|\cos(\theta_T)| \leq 0.7$, where θ_T is the angle between the thrust axis of the three tracks making up the candidate B and the thrust axis of all other tracks and electromagnetic showers in the event. This distribution is flat for $B\bar{B}$ events and peaked at ± 1 for continuum events. These two cuts remove $\geq 99.7\%$ of the continuum, while retaining about 40% of the signal events.

To further reduce continuum backgrounds, we make a cut based on the kinematics of a nonresonant three-body decay [6]. In the rest frame of the B , the angle between the fastest and the second fastest track has a mean value of about 150° . On the other hand, continuum events which fake a B have the topology of two high momentum tracks traveling almost back to back combined with a third low momentum track. Thus we require that the cosine of the angle between the highest momentum and the second highest momentum candidate track be larger than -0.8 , i.e., the angle is $\leq 143^\circ$. This criterion, after applying the cuts in the previous paragraph, keeps about 25% of the signal and only 4% of the remaining continuum background, considerably improving the signal-to-noise ratio. In addition, this requirement removes essentially all contributions due to resonant decays like $B^+ \rightarrow \rho^0 \pi^+, \bar{K}^{*0} \pi^+$, etc. Since the vector particle is produced polarized it emits one track almost back to back with the additional pion, thereby imitating a continuum-like distribution. This cut also removes most of $B^+ \rightarrow D^0 \pi^+, D^0 \rightarrow K^- \pi^+ / \pi^+ \pi^- / K^+ K^-$; the efficiency for the $D\pi$ final state to pass all the above cuts is about $\frac{1}{5}$ that of the three-body signal.

The above mentioned criteria are very efficient at retaining B decays to charmonium final states, e.g., $B^+ \rightarrow \psi K, \psi \rightarrow h^+ h^-$. Since backgrounds from the ψK final state are large and tend to populate the signal region for

the nonresonant final states, we choose to explicitly veto them. To remove instances of $\psi \rightarrow l^+l^-$, we require that none of the three tracks be identified as a lepton. Additional contamination from $B \rightarrow \psi K$ occurs when both leptons are unidentified or when $\psi \rightarrow p\bar{p}, \pi\pi, KK$. Therefore we explicitly remove three-body combinations where any two oppositely charged tracks (analyzed as $\pi^+\pi^-, K^+K^-,$ and $p\bar{p}$) fall within 60 MeV of the ψ mass ($\approx 3\sigma$). Similarly, to remove any remaining $B^+ \rightarrow D^0\pi^+$ decays, we combine opposite sign tracks (as $\pi\pi, KK, K\pi, \pi K$), and veto the combination if it falls within 40 MeV of the D^0 mass ($\approx 3\sigma$).

In three of the decay modes under study ($\pi^+\pi^-K^+, \pi^+\pi^+K^-, K^+K^+K^-$), there is the possibility of feed-through from $B^\pm \rightarrow X_{cc}K^\pm$, where X_{cc} can be $\eta_c, \chi_{c0}, \chi_{c1}, h_c,$ or χ_{c2} , and $X_{cc} \rightarrow \pi\pi$ or KK . Only the $\chi_{c1}K^+$ final state has been measured [7]. The theoretical predictions for the other charmonium states [8] imply that we could have about one to two events coming from these sources in our data sample. Since vetoing all combinations where two oppositely charged tracks have masses falling in the $\chi_c(\eta_c, h_c)$ mass window would drastically reduce the detection efficiency (the selection criteria discussed above preferentially select events in this region of phase space), we choose to make no vetoes on the three $\chi_c, \eta_c,$ and h_c states and accept any feedthrough as nonresonant signal candidates. This procedure makes the upper limits for these nonresonant final states somewhat conservative.

The efficiency for each of the three-body decay modes is estimated using a GEANT [9] based simulation package. The efficiencies for the various decay modes range between 3.6% and 7.1%, as shown in Table I. The error on the efficiency includes our estimate of systematic errors (discussed below).

All the cuts used in this analysis are studied using only Monte Carlo (MC) samples. We use a MC model of signal events to get the number of events surviving various cuts and MC samples of generic $B\bar{B}$ and continuum events to determine backgrounds in the signal region [10]. We choose those cuts which maximize S^2/B .

Since the $Y(4S)$ decays to only two B mesons which are produced almost at rest ($p_B/M_B \approx 0.06$), we constrain the B meson energy to be the same as the beam energy.

This constraint greatly improves the mass resolution of the three-track combination. In addition, we define $\Delta E = (E_1 + E_2 + E_3 - E_{\text{beam}})$, where E_i is the energy of each of the three candidate tracks. We thus define the signal region to be within ± 25 MeV ($\approx 1\sigma$) in ΔE and within 6 MeV ($\approx 2.5\sigma$) of the nominal B mass ($5.28 \text{ GeV}/c^2$). The tight cut on the ΔE region reduces the possibility of cross-feed backgrounds, e.g., $B \rightarrow KK\pi$ feeding into $K\pi\pi$ or KKK .

We do not explicitly account for any cross-feed backgrounds when determining upper limits, e.g., we do not account for true $B \rightarrow K\pi\pi$ decays which may be misidentified as $B \rightarrow \pi\pi\pi$. Since we do not observe signals in any mode, this is not an important consideration. The amount of feed across depends on the decay mode under consideration. For instance, the efficiency for $B \rightarrow \pi\pi\pi$ is about 4.5%, whereas the feed across from $K\pi\pi$ is roughly (0.3–0.6)% depending on whether it is from $K^-\pi^+\pi^+$ or from $K^+\pi^-\pi^+$. In the decays $B \rightarrow \pi^+\pi^+K^-$ and $\pi^+\pi^-K^+$, however, the overlap is of the order of 70%–100%, since ΔE provides little separation.

In Fig. 1, we show the mass distributions for the three track combinations which pass the above mentioned selection criteria (except the cut on the mass) [10]. In each plot, the signal region is between the arrows. There are no discernible signals. In Table I, we present the observed number of events in the signal region. We have also studied the Dalitz plots for all the decay modes and observe no evidence of any feedthrough from charmonium states, e.g., $B^+ \rightarrow \chi_c K^+$.

To estimate backgrounds in the signal region we use a sideband technique. The sideband is defined to be $5.24 \leq M_B \leq 5.29 \text{ GeV}/c^2$ and $|\Delta E| \leq 200$ MeV but outside the signal region. The expected background in the signal region is obtained by scaling the number of events in the combined on-resonance and off-resonance sideband regions; this is also shown in Table I. The scale factors are obtained using generic continuum and $B\bar{B}$ Monte Carlo samples and are obtained by dividing the number of events appearing in the signal region by the number of events in the sideband region. Comparing the data yields with the estimated backgrounds shows that we have no evidence for any significant excess.

TABLE I. Data yields and results.

B^+ Decay mode	Signal yields	Est. bkgd.	Eff. (%)	90% CL upper limit Events	BR(10^{-5})
$\pi^+\pi^+\pi^-$	2	1.2 ± 1.2	4.5 ± 0.66	5.3	4.1
$\pi^+\pi^+K^-$	5	3.9 ± 1.8	4.5 ± 0.66	7.2	5.6
$\pi^+\pi^-K^+$	8	13.0 ± 4.0	7.1 ± 1.10	5.6	2.8
$\pi^+K^-K^+$	14	8.8 ± 3.0	6.7 ± 0.98	14.3	7.5
$K^+K^+K^-$	2	3.9 ± 2.0	3.6 ± 0.54	3.9	3.8
$p\bar{p}\pi^+$	8	8.6 ± 2.4	4.8 ± 0.70	7.2	5.3
$p\bar{p}K^+$	9	4.3 ± 1.5	4.5 ± 0.66	11.4	8.9

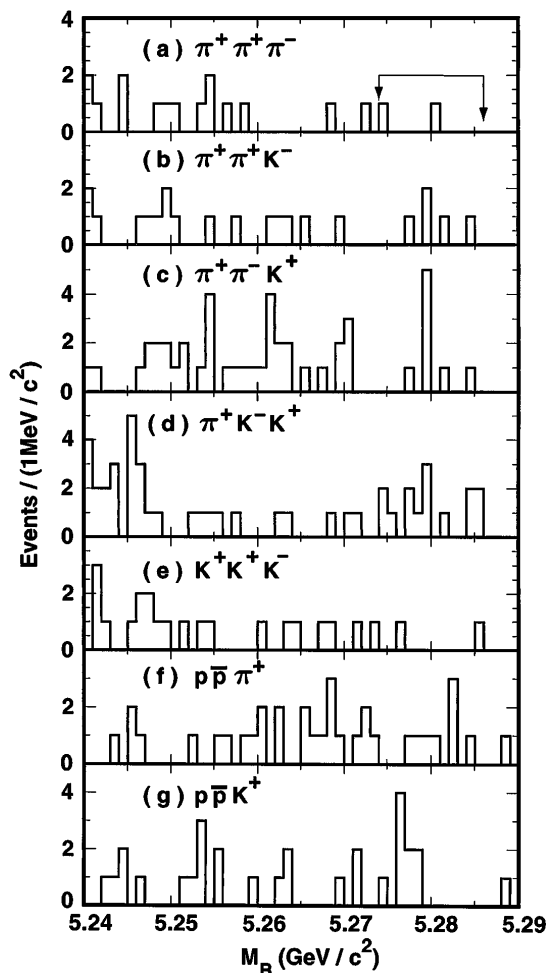


FIG. 1. Mass distributions for (a) $B^+ \rightarrow \pi^+ \pi^+ \pi^-$, (b) $\pi^+ \pi^+ K^-$, (c) $\pi^+ \pi^- K^+$, (d) $\pi^+ K^- K^+$, (e) $K^+ K^+ K^-$, (f) $p \bar{p} \pi^+$, and (g) $p \bar{p} K^+$ candidates. The signal region is between the arrows.

The important issue in this method of estimating backgrounds is that the ratio of events in the signal region and in the sideband agree between data and Monte Carlo. Since we cannot use the signal region in the data sample, we divide the sideband into two regions: (a) sideband one, $5.26 \leq M_B \leq 5.29$ GeV/ c^2 and $|\Delta E| \leq 125$ MeV but outside the signal region, and (b) sideband two, the total sideband region as defined above but outside sideband one. Sideband one is in the im-

TABLE II. Comparison of branching fractions with previous results and theoretical predictions.

B^+ decay Mode	This limit (10^{-5})	Previous best limit (10^{-5})	Theoretical prediction (10^{-5})
$\pi^+ \pi^+ \pi^-$	4.1	5.0 [11]	1.5–8.4 [2]
$\pi^+ \pi^+ K^-$	5.6
$\pi^+ \pi^- K^+$	2.8	19 [12]	...
$\pi^+ K^- K^+$	7.5
$K^+ K^+ K^-$	3.8	20 [13]	...
$p \bar{p} \pi^+$	5.3	8.4 [11]	...
$p \bar{p} K^+$	8.9

mediate vicinity of the signal region and can be thought of as a “pseudosignal” region. The ratios of yields in sidebands one and two agree between data and Monte Carlo; the average values of the ratio of yields in data and MC are 2.6 ± 0.2 and 2.5 ± 0.2 , respectively. This gives us confidence that the ratio of yields between the signal and the total sideband regions will also agree.

To account for the uncertainty in the background estimates, we reduce the background estimate by its error before calculating the upper limit on the signal yield. This error is mainly due to the low statistics involved in determining the scale factors. Similarly we reduce the efficiency by its error before calculating the upper limit on the branching fraction. The error on the efficiency is mainly due to systematic errors. These errors are determined from data wherever possible. Some of the largest contributions to the systematic error are due to particle identification (9%), continuum suppression cuts (6%), error on the tracking efficiency (2% per track), and the tight ΔE cut (4%). We estimate that the total systematic error is about 14% for each mode.

In Table I, we present the 90% confidence level upper limits, which have been calculated using the procedure outlined in the Particle Data Group [7]. The branching fraction upper limits are determined by dividing the upper limits on the yield by the detection efficiency (reduced by 1σ) and the number of produced B^+ and B^- mesons. The present dataset corresponds to $(3.33 \pm 0.07) \times 10^6$ produced B^+ and B^- mesons. We assume equal production of charged and neutral B mesons. A comparison of these upper limits and existing ones is shown in Table II [2,11–13].

In conclusion, we have studied $B^+ \rightarrow h^+ h^+ h^-$ (non-resonant) decays, where h^\pm can be either π^\pm, K^\pm , or $p(\bar{p})$, and present upper limits on their branching fractions. These limits represent a significant improvement over previous limits, and for three of the seven modes studied these are the first published limits. Our limit on $B^+ \rightarrow \pi^+ \pi^+ \pi^-$ branching fraction (4.1×10^{-5}) rules out more than half the range predicted by theory, $(1.5\text{--}8.4) \times 10^{-5}$ [2].

*Permanent address: BINP, RU-630090 Novosibirsk, Russia.

*Permanent address: BINP, RU-630090 Novosibirsk, Russia.

†Permanent address: University of Texas, Austin, Texas.

[1] G. Eilam *et al.*, Phys. Rev. Lett. **74**, 4984 (1995).

[2] N.G. Deshpande *et al.*, Phys. Rev. D **52**, 5354 (1995).

[3] Unitarity of the CKM matrix gives $V_{ud}V_{ub}^* + V_{cd}V_{cb}^* + V_{td}V_{tb}^* = 0$, which describes a triangle in the complex plane. The angles of the triangle are given by $\gamma = \arg(V_{ub}^*)$, $\beta = -\arg(V_{td})$, and $\alpha = \pi - \gamma - \beta$, in the Wolfenstein parameterization. L. Wolfenstein, Phys. Rev. Lett. **51**, 1945 (1983).

[4] CLEO Collaboration, Y. Kubota *et al.*, Nucl. Instrum. Methods Phys. Res., Sect. A **320**, 66 (1992).

-
- [5] G. Fox and S. Wolfram, *Phys. Rev. Lett.* **41**, 1581 (1978).
- [6] We assume that a nonresonant three-body decay has a constant matrix element across phase space.
- [7] Particle Data Group, L. Montanet *et al.*, *Phys. Rev. D* **50**, 1173 (1994).
- [8] J. H. Kühn *et al.*, *Z. Physik C* **5**, 117 (1980); G. T. Bodwin *et al.*, *Phys. Rev. D* **46**, 3703 (1992).
- [9] R. Brun *et al.*, Report No. GEANT 3.15, CERN DD/EE/84-1. The generator used in the CLEO Monte Carlo calculations agree well with data when comparing features such as particle momenta spectra, multiplicities, etc.
- [10] Each event in the data or generic Monte Carlo sample can contribute to more than one decay mode.
- [11] ALEPH Collaboration, in Proceedings of the International Conference on High Energy Physics, Warsaw, 1996 (Report No. PA-05-057).
- [12] CLEO Collaboration, P. Avery *et al.*, *Phys. Lett. B* **223**, 470 (1989).
- [13] DELPHI Collaboration, W. Adam *et al.* (to be published).